Barker, P.F., Camerlenghi, A., Acton, G.D., and Ramsay, A.T.S. (Eds.)
Proceedings of the Ocean Drilling Program, Scientific Results Volume 178

3. Sediment Color Variation and Annual Accumulation Rates in Laminated Holocene Sediments, Site 1098, Palmer Deep[1]

Alexandra J. Nederbragt[2] and Juergen Thurow[2]

ABSTRACT

Continuous sediment color records with a resolution of one measurement per millimeter were generated for Site 1098 (Palmer Deep, Antarctic Peninsula) from digital images of the core surfaces to test if the laminated intervals at this site will allow for analysis of high-frequency climate variability in the Circum-Antarctic. Long-term variation in color values correlates with gamma-ray attenuation bulk density. Darker colors are found in laminated intervals with lower bulk density, high biogenic silica, and high total organic carbon content. Darker color values result from the addition of dark laminae to background sediments that show little variation in color. The thicknesses of dark and light laminae were measured in the top 25 meters composite depth to determine the temporal resolution of the laminae. The alternation between dark, biogenic-rich laminae and background sediment essentially represents an annual cycle, but the sediment is not consistently varved. The modal thickness of light laminae is close to the long-term average annual accumulation rate, and results indicate that approximately half of the dark/light couplets in distinctly laminated intervals represent a single year. Missing biogenic laminae are interpreted to represent reduced primary productivity during cold years with delayed breakup of the sea-ice cover.

[1]Nederbragt, A.J., and Thurow, J., 2001. Sediment color variation and annual accumulation rates in laminated Holocene sediments, Site 1098, Palmer Deep. *In* Barker, P.F., Camerlenghi, A., Acton, G.D., and Ramsay, A.T.S. (Eds.), *Proc. ODP, Sci. Results,* 178, 1–20 [Online]. Available from World Wide Web: <http://www-odp.tamu.edu/publications/178_SR/VOLUME/CHAPTERS/SR178_03.PDF>. [Cited YYYY-MM-DD]
[2]Department of Geological Sciences, University College London, Gower Street, London WC1E 6BT, United Kingdom. Correspondence author: **a.nederbragt@ucl.ac.uk**

Initial receipt: 14 August 2000
Acceptance: 5 February 2001
Web publication: 29 May 2001
Ms 178SR-209

INTRODUCTION

Ocean Drilling Program (ODP) Site 1098 in the Palmer Deep, Antarctic Peninsula (Fig. F1) offers the potential to reconstruct a high-resolution record of marine Holocene climate in the Antarctic. A ~50-m-thick Holocene sequence of intermittently laminated diatom oozes and diatom-bearing muds was recovered at this site (Barker, Camerlenghi, Acton, et al., 1999). Sediments in the Palmer Deep document centennial-scale variation in marine productivity, expressed as meter-scale alternations between homogeneous bioturbated levels and laminated intervals with increased biogenic silica (Leventer et al., 1996; Domack et al., in press). Within the laminated intervals, light sediments alternate with diatom-rich laminae that are generally darker than the surrounding sediment. The diatom-rich laminae represent a seasonal signal of high productivity and/or diatom blooms (Leventer et al., 1996; Barker, Camerlenghi, Acton, et al., 1999; Pike et al., **Chap. 18,** this volume). The laminated portions of the Site 1098 record are therefore potentially varved and may offer the temporal resolution to reconstruct the extent of (sub)decadal climate variability in the Circum-Antarctic.

A correlation between increased diatom content and darker color implies that sediment color is a suitable proxy to compile such a high-resolution climate record, as color is a sediment property that can be measured easily. However, the shipboard color measurements generated with a Minolta spectrophotometer (Barker, Camerlenghi, Acton, et al., 1999) are based on one discrete measurement every 2 cm, a resolution too coarse to resolve color variation within the dark/light couplets. In addition, meter-scale cycles are also difficult to recognize (Acton et al., **Chap. 5,** this volume) because of scatter in the data resulting from undersampling of the centimeter-scale variation in color. In contrast, digital images of sediment surfaces, which we collected on shore after the cruise, provide the means to compile color records with the spatial resolution necessary to register lamina-scale color variation. Such ultrahigh-resolution time series have been used to unravel climatic history on annual to centennial scales represented in annually laminated sediments (Merrill and Beck, 1995; Schaaf and Thurow, 1995; Nederbragt and Thurow, in press). Here, we explore whether the continuous color time series derived from digital images provides a suitable proxy to describe variation in sediment composition at Site 1098. We also compare laminae thickness variation with published radiocarbon ages (Domack et al., in press) to determine the temporal resolution of the dark/light couplets to test whether laminated intervals are varved.

F1. Map showing the location of ODP Site 1098, p. 10.

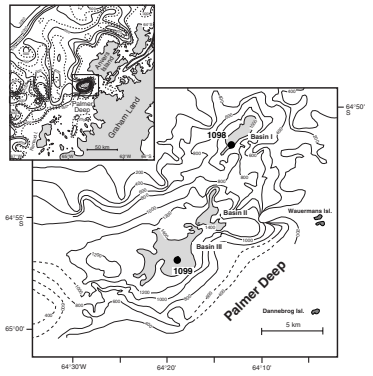

METHODS

Digital images of split-core surfaces of sediments from Holes 1098A, 1098B, and 1098C were collected at the ODP Core Repository in Bremen, Germany, before postcruise sampling was done, as it spoils core surfaces for imaging purposes. Images were generated with a digital color line-scan camera mounted on a Geotek multisensor track. The camera is fixed and collects line scans of 980 pixels across the core surface for each of the three colors separately (red, green, and blue [RGB]) while the core is pushed along the rack by a motor. Individual line scans are compiled into blocks of 2048 lines and stored as one image. Given the speed at which the core was moved underneath the camera, each 980 pixel × 2048 pixel image has a theoretic stratigraphic resolu-

tion of ~120 pixels/cm. However, the camera was still in an experimental phase when the Site 1098 cores were scanned and part of the time it produced darker stripes overlaid over the real sediment color variation. These stripes, when present, have a regular wavelength of 11 pixels (0.92 mm of sediment) and limit the effective resolution of the images to ~1 mm. This resolution is still fine enough to describe the color variation within the laminated intervals of Site 1098, as dark/light couplets are generally >4 mm thick.

Images include a cloth centimeter scale that was draped on the sediment surface along the edge of the core to translate the pixel positions into a metric scale. A Kodak color reference card was scanned after each 1.5-m section to allow for calibration of color values and for correction of any-long term variation in the light source. Core surfaces were scraped carefully before scanning to smooth sediment surface as best as possible. Scratches in the sediment or other surface irregularities produce dark shadows and/or light reflections, which introduce artifacts in the registered color values in the digital image. All undisturbed pelagic intervals in all three holes were scanned. Excluded are intervals with physically disturbed sediments (core catchers, except Sample 178-1098B-5H-CC, and the top 30-60 cm of each core) (Acton et al., **Chap. 5,** this volume) and the central portion of the thick, homogeneous turbidite between 25 and 29 meters composite depth (mcd) (Barker, Camerlenghi, Acton, et al., 1999).

Nederbragt et al. (2000) described the methods used to extract a line scan of RGB color values from each image and to translate those into L*a*b* values using a color reference card for calibration. In the L*a*b* system defined by the Commission Internationale de l'Éclairage, L* represents lightness, ranging between 0 = black and 100 = white. The other two variables describe the actual color, with a* representing green (negative values) or red (positive values) and b* representing blue (negative values) or yellow (positive values). Color values were extracted from a 20-pixel-wide strip (= 2 mm) along the stratigraphic axis in individual images and compiled into a continuous color record. The data were subsequently filtered to remove the millimeter-scale dark stripes produced as an artifact by the camera. To that purpose, a low-pass filter was applied in the frequency domain to remove all variation with wavelengths of 1 mm and less. The files were then reduced in size to one L*, a*, and b* value per millimeter by taking the median value in each millimeter interval. An average value per centimeter interval is used to describe long-term variation in color (Tables **T1, T2, T3**). All images were logged visually on the computer screen to measure the thickness and stratigraphic position of dark laminae, using the image analysis package NIH-Image, in combination with a macro that translates subsequent mouse clicks on the image into stratigraphic position.

The depth-age relation used here is based on the published composite depth scheme (Acton et al., **Chap. 5,** this volume) and radiocarbon ages (Domack et al., in press). Minor modifications are made to the composite depth scale. An abrupt shift in radiocarbon ages indicates that erosion occurred below the second 1.2-m-thick turbidite, at ~33 mcd (Domack et al., in press). In Core 178-1098C-4H, more sediment appears to have been removed than in the other two holes. The best match with the other two holes of the top of Core 178-1098C-4H and the lower part of the core is obtained when a gap of 62 cm is introduced below the base of the turbidite at interval 178-1098C-4H-3, 60 cm (Fig. **F2**). This match is based on whole-core magnetic susceptibility records, which show a good correlation in this interval (Acton et al., **Chap. 5,**

T1. Hole 1098A digital image color data, p. 18.

T2. Hole 1098B digital image color data, p. 19.

T3. Hole 1098C digital image color data, p. 20.

F2. Sediment lightness at Site 1098 vs. modified composite depth, p. 11.

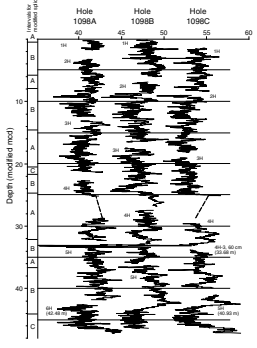

this volume). Color (Fig. F2) and gamma-ray attenuation (GRA) bulk density show more lateral variation in this interval. The composite depth scale is also changed for Cores 178-1098A-6H and 178-1098C-5H to obtain a best-fit match for the pattern of color variation within the distinctly laminated interval at the base of Site 1098. A modified splice was constructed to sample the most representative color-variation record (Fig. F2).

RESULTS

Color and Sediment Composition

The Holocene section at Site 1098 shows clear meter-scale variation between darker and lighter sediments (Figs. F2, F3). The pattern of variation in color is continuous laterally in the distinctly laminated sediments between 0 and 25 mcd and between 42.5 and 46 mcd. Color variation between 28 and 42 mcd cannot be correlated between holes (Fig. F2). Lateral changes in sediment color in this interval may be the result of variable bioturbation with the presence of discrete burrows. However, decimeter- to meter-scale fluctuations in sediment color throughout the record match with variation in bulk density (Fig. F3). Leventer et al. (1996) showed for a piston core from the same locality as Site 1098 that, in the upper 10 meters below seafloor, laminated intervals have lower bulk density and higher biogenic silica content than bioturbated levels. The average darker colors in intervals with lower bulk density (high biogenic silica) are mainly the result of the presence of bundles of darker laminae (Fig. F3). Color values of the light laminae are similar to those in the bioturbated homogeneous intervals, representing background sediments that show relatively little variation in lightness (Fig. F4). The dark laminae have variable lightness, ranging from dark to a value that is only slightly darker than the background sediment, and have variable color values, ranging between gray, olive, and orange-brown (Barker, Camerlenghi, Acton, et al., 1999). Yet, dark laminae are commonly rich in diatoms, which causes a decrease in bulk sediment density. As a result, the linear correlation between GRA bulk density and L* (r = 0.46) is significant but not very high. Although variation in a* is low amplitude, a* is highly negatively correlated with lightness (r = –0.84), that is, darker sediments are more red. A lower correlation between L* and b* (r = –0.42) indicates that dark sediments have a more variable yellow component.

The sequence at Site 1098 contains two intervals that both have a high proportion of laminated sediments but differ in sedimentological characteristics. The interval from the top of the sequence to 25 mcd shows cyclic alternation between laminated and bioturbated sediments. The transition between dark and light laminae is gradual. Laminae occur in bundles that can be traced across all three holes (Fig. F4). Within these bundles, most individual laminae are also continuous (Fig. F5). Variation between cores appears in part a result of physical disturbance of the primary lamination, possibly caused by the coring of the very weakly consolidated sediments. The overall lateral continuity of individual laminae and the gradual transitions between dark and light are consistent with quiet deposition from pelagic rain, with dark laminae representing settling of biogenic fluxes during the growing season.

The lower interval between ~42.5 and ~46 mcd is more continuously laminated than the top 25 mcd but shows much more lateral variability

F3. Color variables for the spliced record vs. density and number of dark laminae, p. 12.

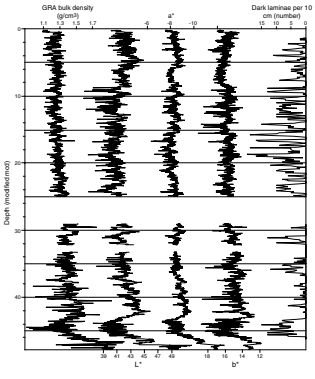

F4. Detail of L* trends in all three holes between 13 and 15.5 mcd, p. 13.

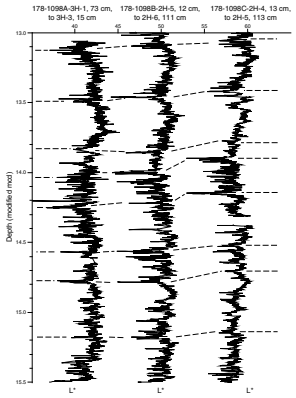

F5. Image data for Holes 1098B and 1098C, p. 14.

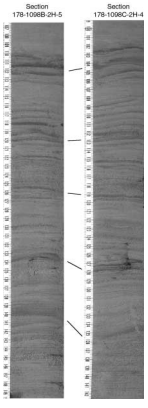

(Figs. F6, F7). Laminae in Hole 1098A show high-amplitude color variation, and dark levels tend to be thick and have sharp boundaries with the surrounding lighter sediments. In Holes 1098B and 1098C, dark laminae are mostly thinner with more gradual transitions in color, but the sequence is tilted and shows signs of slumping and/or erosion in several places. Meter-scale fluctuations in average color in this part of the sequence appear to correlate between the three holes, but individual laminae cannot be traced laterally, except between Holes 1098B and 1098C between 44 and 45.6 mcd (Figs. F6, F7). Backscatter electron microscope images of impregnated sediments show indications of redeposition of diatom floras (Pike et al., Chap. 18, this volume). Overall, the lack of lateral continuity indicates that the laminated interval between ~42.5 and ~46 mcd cannot be interpreted as a continuous pelagic drape, as it shows signs of disturbance, possible discontinuities, and appears influenced by current action.

Accumulation Rates

The combination in the upper 25 mcd of high accumulation rates (~4 mm/yr) (Domack et al., in press) and lateral continuity of laminae with the fact that biogenic productivity occurs during a short season suggests that laminated intervals could be varved, that is, dark/light couplets could represent a single year. If that were the case, then annual-resolution age scales could be produced simply through counting varves in the best laminated intervals. To explore the amount of time represented between pairs of dark laminae, we measured the thickness of all dark laminae and all light intervals in between. For dark/light couplets, we added the thickness of each light interval to that of the overlying dark lamina, irrespective of the thickness of the light interval. We concentrate on the upper 25 mcd, which we interpret as pelagic, and for which a detailed radiocarbon age scale is available (Domack et al., in press).

The thickness of virtually all dark/light couplets throughout the upper 25 mcd exceeds the long-term average annual accumulation rates derived from radiocarbon measurements (Fig. F8). This does not necessarily mean that dark/light couplets on average represent more than a single year. Leventer et al. (1996) concluded that laminated intervals represent higher-than-average total accumulation rates, through the addition of increased diatom fluxes. In addition, the thickness of dark and biogenic-rich laminae is highly variable, ranging from 0.1 to >1.0 cm (mean = 0.34 cm, standard deviation = 0.29). Given that the composition of the biogenic-rich laminae is consistent with deposition during a single growing season, the variation in thickness indicates extreme interannual variation in biogenic fluxes. We conclude that the fact that most dark/light couplets are thicker than the expected long-term average annual flux reflects primarily a distinct increase in total biogenic sediment accumulation rates in the laminated intervals relative to the homogenous levels.

This conclusion suggests as an alternative model for sedimentation that terrigenous fluxes remained relatively constant through time, whereas biogenic fluxes were highly variable. As a first-order approximation, we equate dark laminae with biogenic event deposition and light levels with siliciclastic background sedimentation. Radiocarbon accumulation rates were therefore recalculated for the light sediments only after subtracting all dark laminae from the total sediment thickness. The result shows a long-term average annual rate of deposition of

F6. Detail of L* trends in all three holes between ~43 and 46 mcd, p. 15.

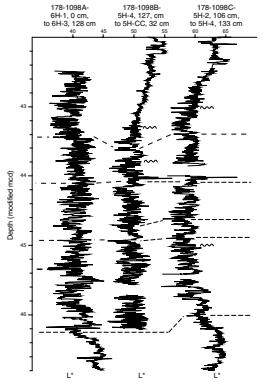

F7. Image data for Holes 1098A, 1098B and 1098C, p. 16.

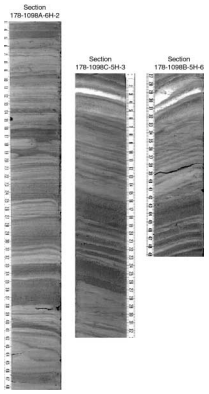

F8. Thicknesses of dark/light couplets and light intervals vs. average sediment accumulation rates, p. 17.

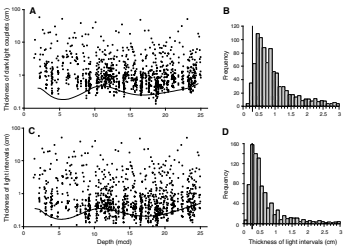

light sediment that is close to the mode in thickness of light-colored laminae (Fig. F8D). This indicates that a large number of the dark/light couplets indeed represent a single year. However, the highly skewed distribution of light laminae thickness also indicates that an equally large number of light layers in the 0.5 to 2.0 cm range are too thick to represent a single year. We assume that annual rates of accumulation have a normal distribution, with the mean given by the long-term radiocarbon-based rate and a standard deviation estimated from the left side of the histogram in Figure F8D. We can then estimate the expected number of annual layers thicker than the mean. The result indicates that out of a total of 823 light laminae in the spliced record some 460 represent deposition over two or more years. Although a rough estimate, it suggests strongly that there are many "missing years" even within the best laminated intervals, that is, years that a biogenic layer was not deposited or, if deposited, not preserved as a recognizable laminae.

DISCUSSION AND CONCLUSIONS

The color-time series presented here shows that sediment color provides a useful variable to describe the Site 1098 sediments. Digital images can be used to describe gradual color changes at decimeter scale (Nederbragt et al., 2000), but the Minolta photospectrometer is less labor-intensive in such a case. In laminated sediments, however, digital images not only have the resolution to register within-lamina variation but also allow long-term trends to be described more reliably. Problems in correlating the shipboard Minolta photospectrometer measurements with other records (Acton et al., Chap. 5, this volume) result from stochastic scatter resulting from inadequate sampling of the centimeter-scale color variation. The Minolta records are spiky, with large fluctuations dependent on whether the measurement was in a dark or light lamina. The continuous time series derived from image data have the advantage that color can be integrated over a given interval to produce average values. With the strong and rapid color variation within the laminated intervals at Site 1098, such image-derived averages yield a smoother long-term trend that matches well with other sediment variables like GRA bulk density (Fig. F3).

Color variation at the decimeter to meter scale correlates significantly with sediment density, but the linear correlation coefficient is not very high (Fig. F3). Data to correlate sediment color with sediment chemistry at Site 1098 are not available yet. However, marine sediments in other areas showed that color reacts most strongly to variation in carbonate and total organic carbon (TOC) content; any correlation between biogenic silica content and color is usually weak and dependent on overall sediment composition and mineralogy of the terrigenous component (Nederbragt et al., 2000). TOC content reaches values of up to 1.5 wt% in the upper 10 m of the sediment column in Palmer Deep (Leventer et al., 1996), that is, values that are high enough to have a clear effect on sediment color. With biogenic silica and terrigenous material forming the bulk of the sediment, GRA bulk density and magnetic susceptibility should primarily measure the ratio between these two components. Visual inspection of the sediments at Site 1098 indicates that sediment color and diatom content are partly independent of each other. Dark laminae are usually diatom rich, but the reverse is not true. Many diatom-rich intervals do not clearly differ in color from surrounding, more terrigenous sediments and presumably are not en-

riched in organic carbon. A factor that will contribute to a weak correlation between silica and TOC is that a large number of biogenic silica–rich laminae consist of diatom resting spores, which are formed under low-productivity conditions in response to nutrient depletion (Leventer et al., 1996; Pike et al., **Chap. 18,** this volume). We expect a further study to show that color traces TOC content primarily, that GRA bulk density is mostly a function of biogenic silica content, and that the relatively weak correlation between the two is the result of a partly nonlinear relation between export fluxes of diatoms and organic matter.

Whereas sediment color has potential as a meaningful proxy, the second requirement for analysis of high-frequency climate cycles, an accurate age scale with annual resolution, may be difficult to realize. Conditions in Palmer Deep are favorable for the formation of varved sequences, given the high average accumulation rates, the strong seasonal limitation of biogenic productivity, and the lack of bioturbation under anoxic conditions. The close match of long-term accumulation rates of light sediments with the modal thickness of light laminae (Fig. **F8**) indicates that many dark/light couplets indeed represent an annual cycle. However, there are too many "missing" dark laminae to classify the laminated intervals as varved. It is therefore not feasible to simply use laminae counts to establish a reliable (floating) age scale. Part of the missing dark laminae could represent light intervals in which a thin diatom-rich level is preserved but not visible in color change. However, given the large variation in thickness of recognizable dark laminae ranging between <1 mm and >1 cm, it seems likely that the range of variation includes the virtually complete absence, or nonpreservation, of biogenic productivity during some years.

We attribute the extreme interannual variability in marine productivity primarily to variation in temperature around the Antarctic peninsula. Instrumental records for the past 20 yr show the presence of loose sea ice in Palmer Deep, usually from February to May, but even the short available records show considerable interannual variation (Stammerjohn and Smith, 1996). Leventer et al. (1996) relate high biogenic silica fluxes to periods during which a stratified water column with nutrient depletion in the upper water is generated, inducing the formation of diatom resting spores or diatom mats that sink more easily to the seafloor. One variable that is not addressed in this interpretation is the length of time that primary producers can grow as a result of light limitation. Without sea ice, spring blooms in the Southern Hemisphere would be expected to start around October, when days start to lengthen. The presence of a sea-ice cover until much later in the solar year must cause sunlight to be biolimiting until the ice has broken up, leaving only a short growing season. We expect that the large variation in the total annual biogenic flux in Palmer Deep is primarily a function of Antarctic temperature. In warm years, the sea-ice cover would break up earlier, giving a growing season long enough for primary producers to deplete nutrients in the photic zone, whereas only thin biogenic layers would be formed during colder-than-average years, when delayed ice breakup causes lack of sunlight to be a major biolimiting factor.

ACKNOWLEDGMENTS

We are grateful to U. Röhl for allowing us to use the Geotek camera scanner at the University of Bremen and to W. Hale and A. Wülbers for

their help during our visit to the Bremen ODP Core Repository. This study is supported by NERC grant GST/02/2525.

REFERENCES

Barker, P.F., Camerlenghi, A., Acton, G.D., et al., 1999. *Proc. ODP, Init. Repts.,* 178 [CD-ROM]. Available from: Ocean Drilling Program, Texas A&M University, College Station, TX 77845-9547, U.S.A.

Domack, E., Leventer, A., Dunbar, R., Taylor, F., Brachfeld, S., Sjunneskog, C., and ODP Leg 178 Science Party, in press. Chronology of the Palmer Deep Site, Antarctic Peninsula: A Holocene Paleoenvironmental Reference for the Circum-Antarctic. *The Holocene.*

Leventer, A., Domack, E.W., Ishman, E., Brachfeld, S., McClennen, C.E., and Manley, P., 1996. Productivity cycles of 200–300 years in the Antarctic Peninsula region: understanding linkages among the sun, atmosphere, oceans, sea ice, and biota. *Geol. Soc. Am. Bull.,* 108:1626–1644.

Merrill, R.B., and Beck, J.W., 1995. The ODP color digital imaging system: color logs of Quaternary sediments from the Santa Barbara Basin, Site 893. *In* Kennett, J.P., Baldauf, J.G., and Lyle, M. (Eds.), *Proc. ODP, Sci. Results,* 146 (Pt. 2): College Station, TX (Ocean Drilling Program), 45–59.

Nederbragt, A.J., and Thurow, J., in press. A 6000 year varve record of Holocene climate in Saanich Inlet, British Columbia, from digital sediment colour analysis of ODP Leg 169S cores. *Mar. Geol.*

Nederbragt, A.J., Thurow, J.W., and Merrill, R.B., 2000. Data report: Color records from the California margin: proxy indicators for sediment composition and climatic change. *In* Lyle, M., Koizumi, I., Richter, C., and Moore, T.C. (Eds.), *Proc. ODP, Sci. Results,* 167: College Station, TX (Ocean Drilling Program), 319–329.

Schaaf, M., and Thurow, J., 1995. Late Pleistocene–Holocene climatic cycles recorded in Santa Barbara Basin sediments: interpretation of color density logs from Site 893. *In* Kennett, J.P., Baldauf, J.G., and Lyle, M. (Eds.), *Proc. ODP, Sci. Results,* 146 (Pt. 2): College Station, TX (Ocean Drilling Program), 31–44.

Stammerjohn, S.E., and Smith, R.C., 1996. Spatial and temporal variability in west Antarctic sea-ice coverage. *Am. Geophys. Union, Antarct. Res. Ser.,* 70:81–104.

Figure F1. Map showing the location of ODP Site 1098 (from Acton et al., Chap. 5, this volume).

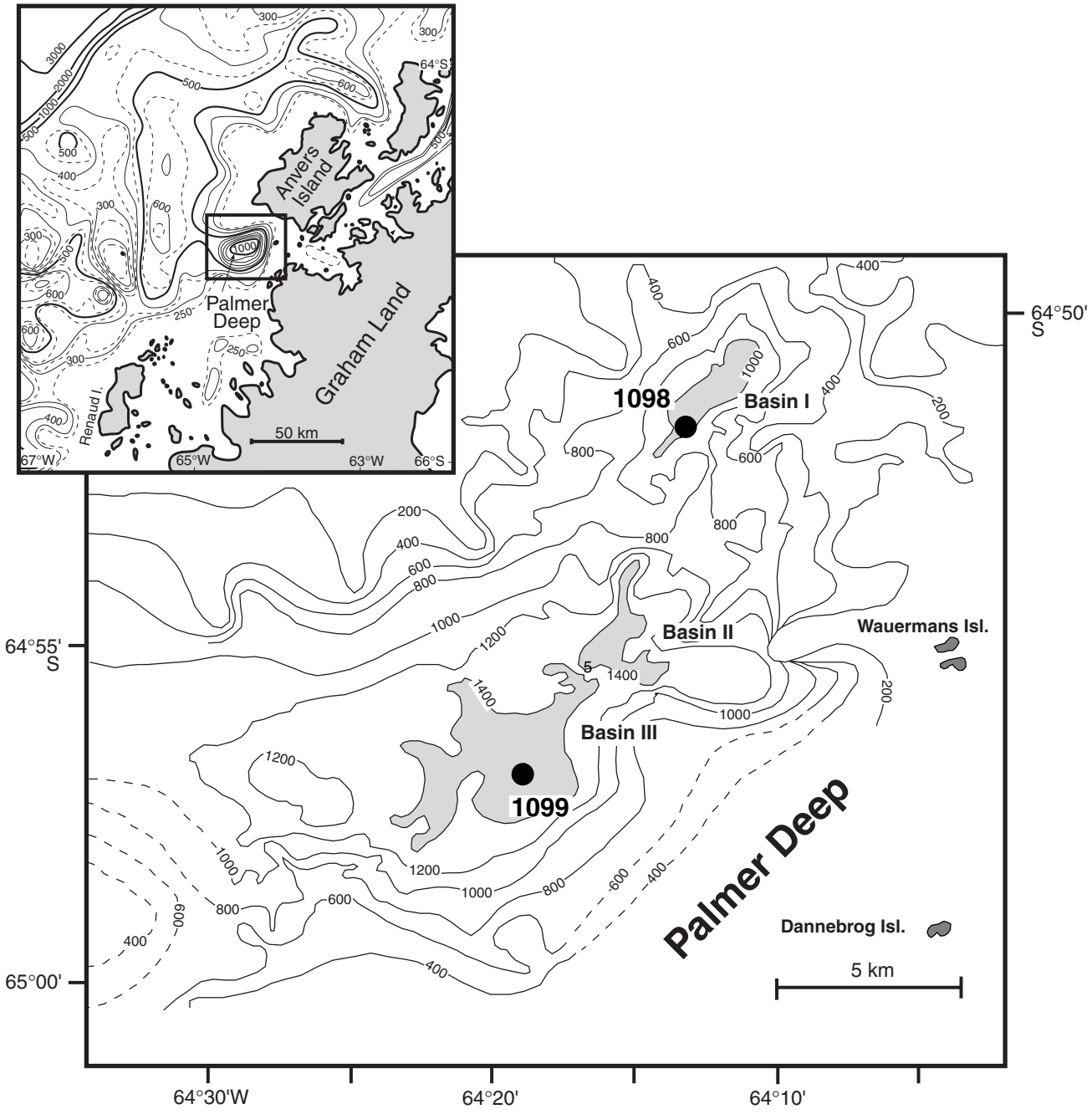

Figure F2. Sediment lightness (L*) in Holes 1098A, 1098B, and 1098C plotted against modified composite depth. L* data were summarized into one integrated value per centimeter and then smoothed with a 3-point running average. Note that Holes 1098B and 1098C are offset by 6 and 12 units, respectively. The composite depth scale is that of Acton et al. (**Chap. 5,** this volume), except for Cores 178-1098A-6H and 178-1098C-5H and the interval below 178-1098C-4H-3, 60 cm, with modified depths given on the plot. A modified splice used in this study is indicated graphically in the column on the left, where letters indicate which hole was used for each interval. The gap in L* data around 26–28 mcd represents the central portion of the topmost turbidite in Holes 1098A and 1098C, which was not included in the digital image data set.

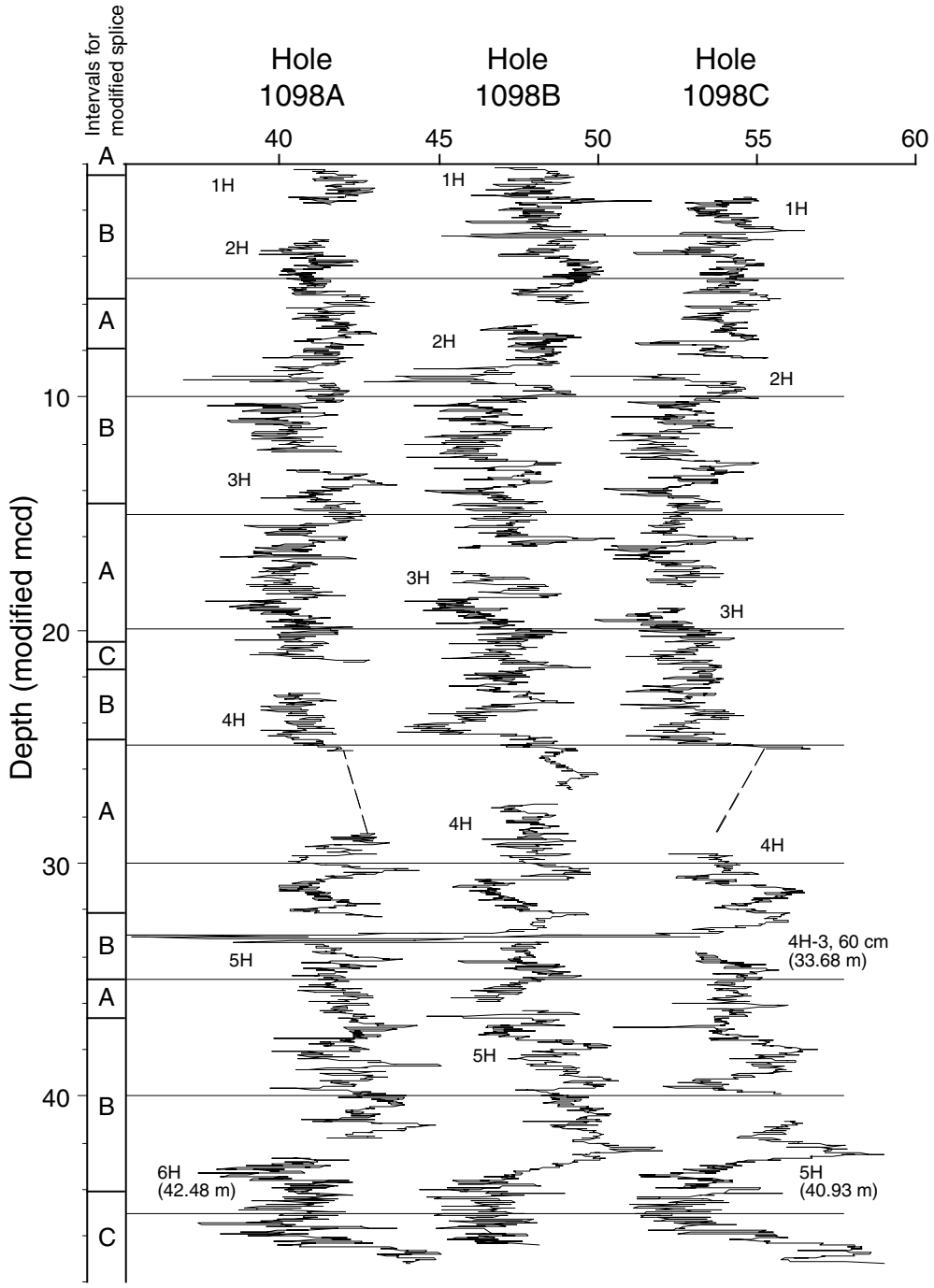

Figure F3. Color variables for the spliced record as in Figure F2, p. 11, compared to shipboard GRA bulk density measurements and the number of dark laminae counted in each 10-cm interval. To allow estimation of product moment correlation coefficients, color variables were calculated as the average value in a centimeter interval centered around the GRA measurements. Correlation coefficients of GRA bulk density with L* = 0.46, of a* with L* = –0.84, and of b* with L* = –0.42. Note that scales of a*, b*, and number of laminae are inverted to facilitate visual comparison of trends and that turbidites between ~25 and ~29 mcd and ~32 and ~33 mcd are not included in the data.

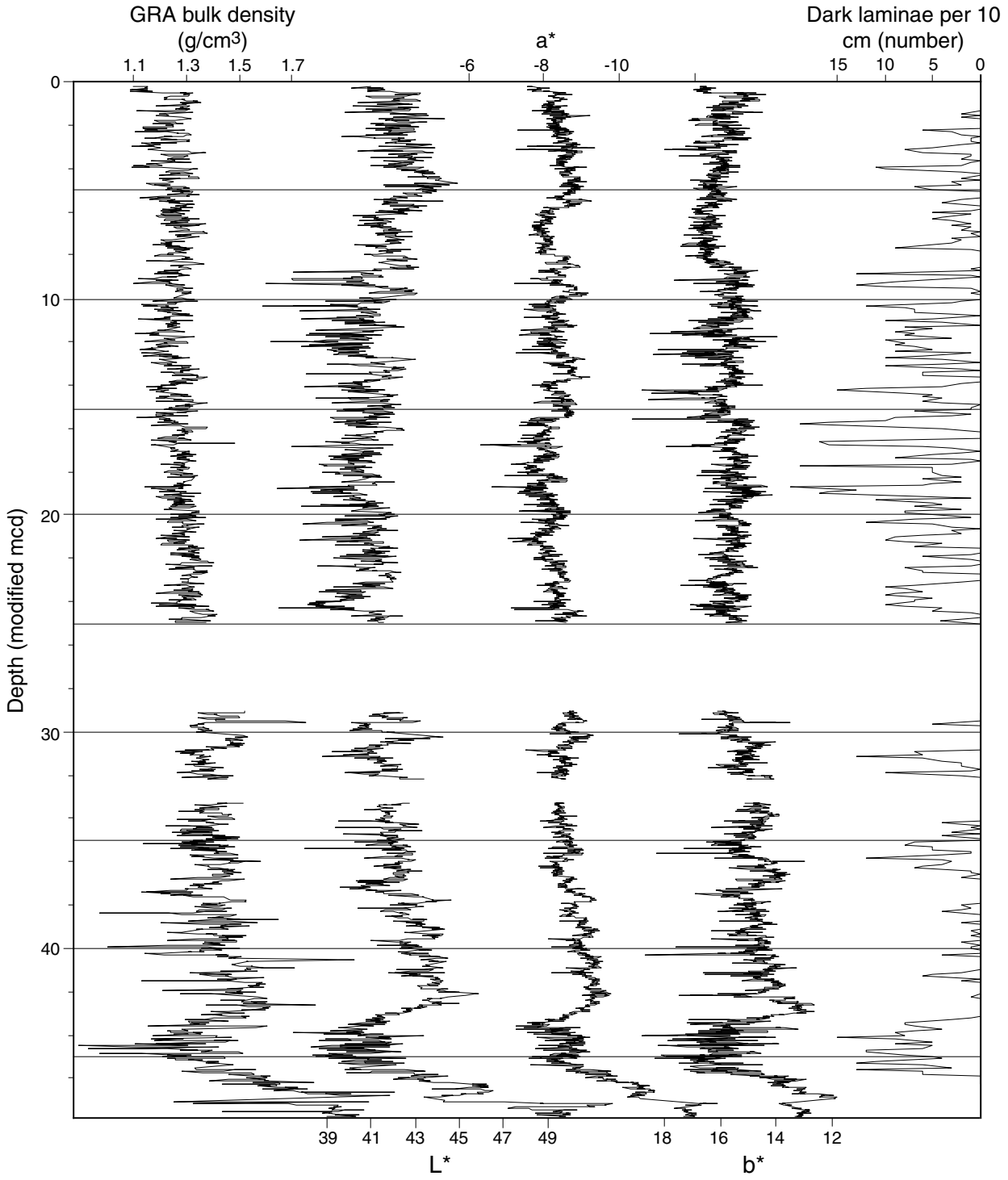

Figure F4. Detail of L* trends in all three holes between 13 and 15.5 mcd as a representative example of the record between 0 and 25 mcd, showing lateral continuity of bundles of laminae. Plotted are the 1-mm-resolution L* time series after smoothing with a 3-point moving average. Dotted lines trace the correlation of individual laminae between holes.

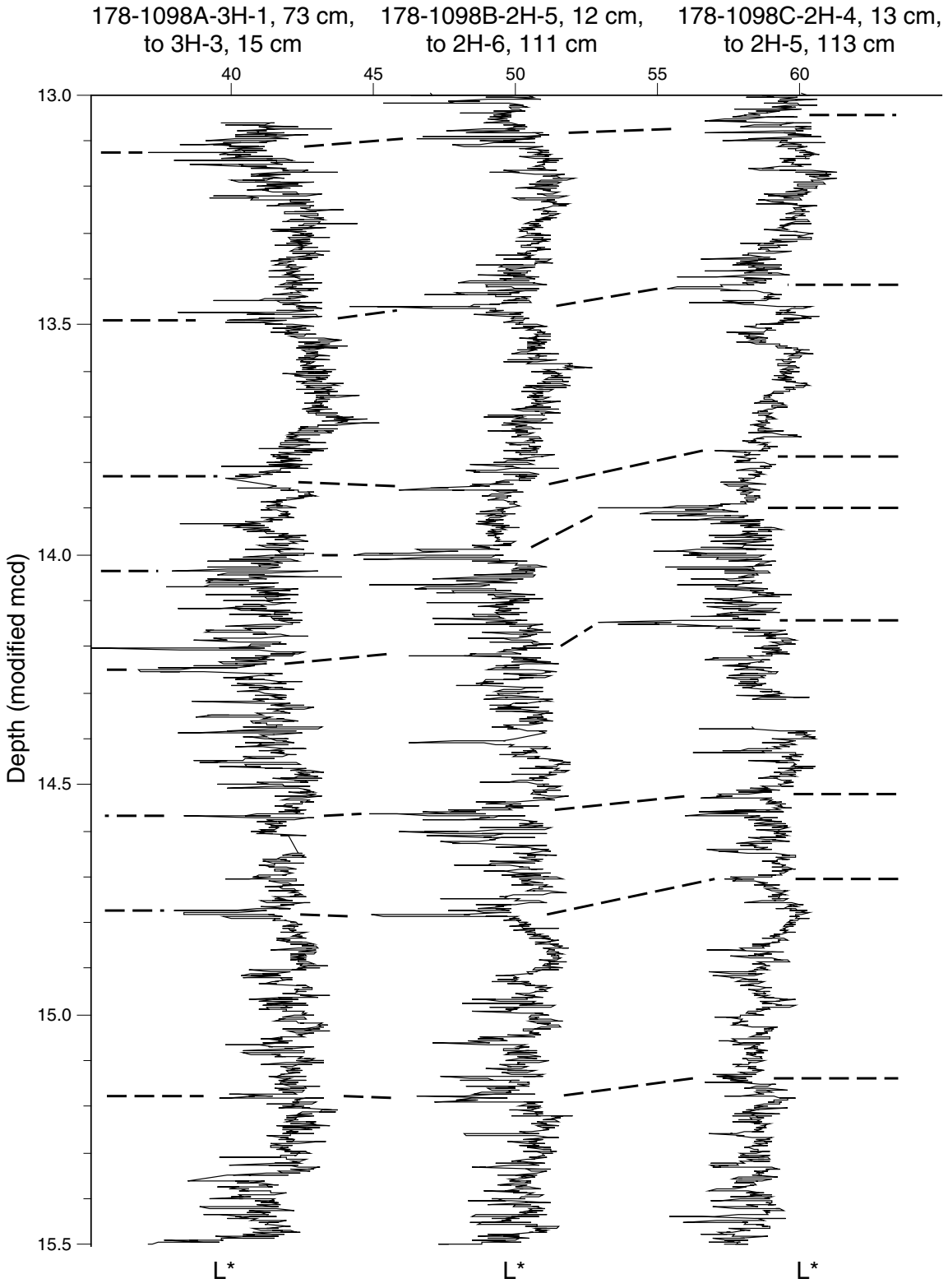

Figure F5. Image data for Holes 1098B and 1098C, corresponding to the interval between 14.0 and 14.4 mcd in Hole 1098B in Figure F4, p. 13, showing that most individual dark laminae can be traced between holes. Note that images are a gray-scale translation of the original color files, and that contrast and brightness are enhanced.

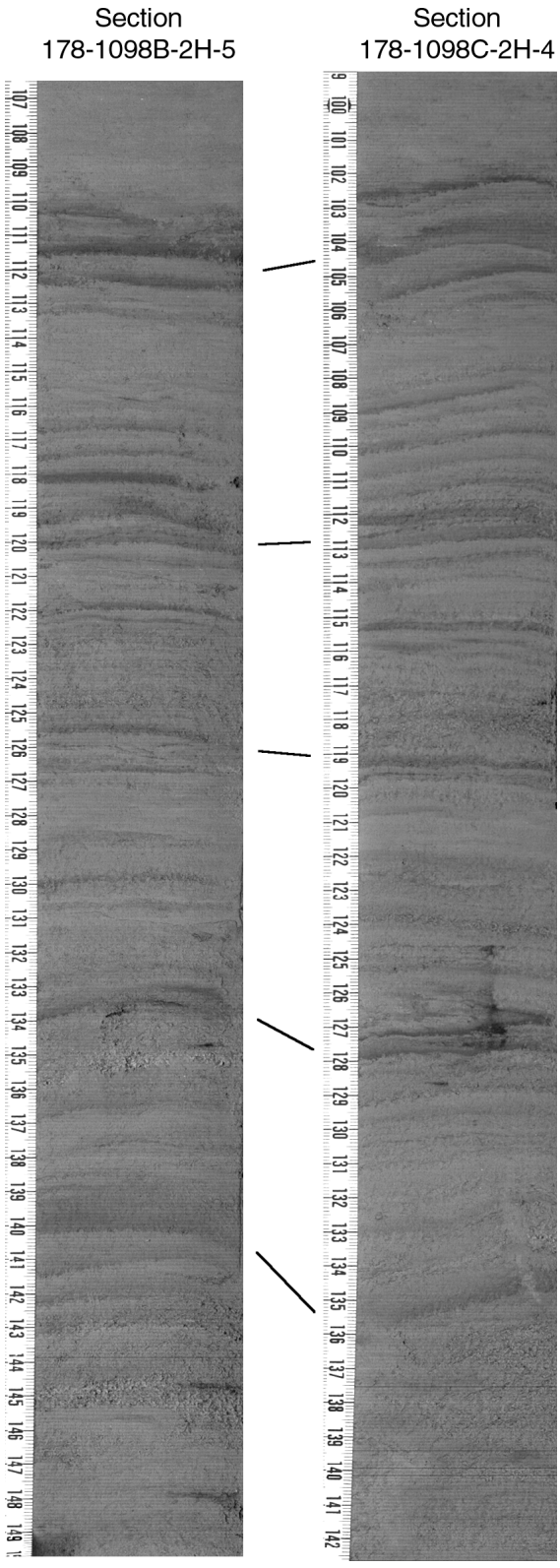

Figure F6. Detail of L* trends in all three holes for the laminated interval between ~43 and 46 mcd. Note that all three holes have similar long-term trends in sediment lightness, but that a good correlation between individual laminae is possible only for Holes 1098B and 1098C in the interval between 44.1 and 45.5 mcd. Plotted are the 1-mm-resolution L* time series after smoothing with a 3-point moving average; gaps between sections in Hole 1098C correspond to whole-core interstitial water samples. Dotted lines trace the correlation of long-term (≥10 cm) variation in color; wavy lines show the position of possible discontinuities as indicated by slump features or angular disconformities.

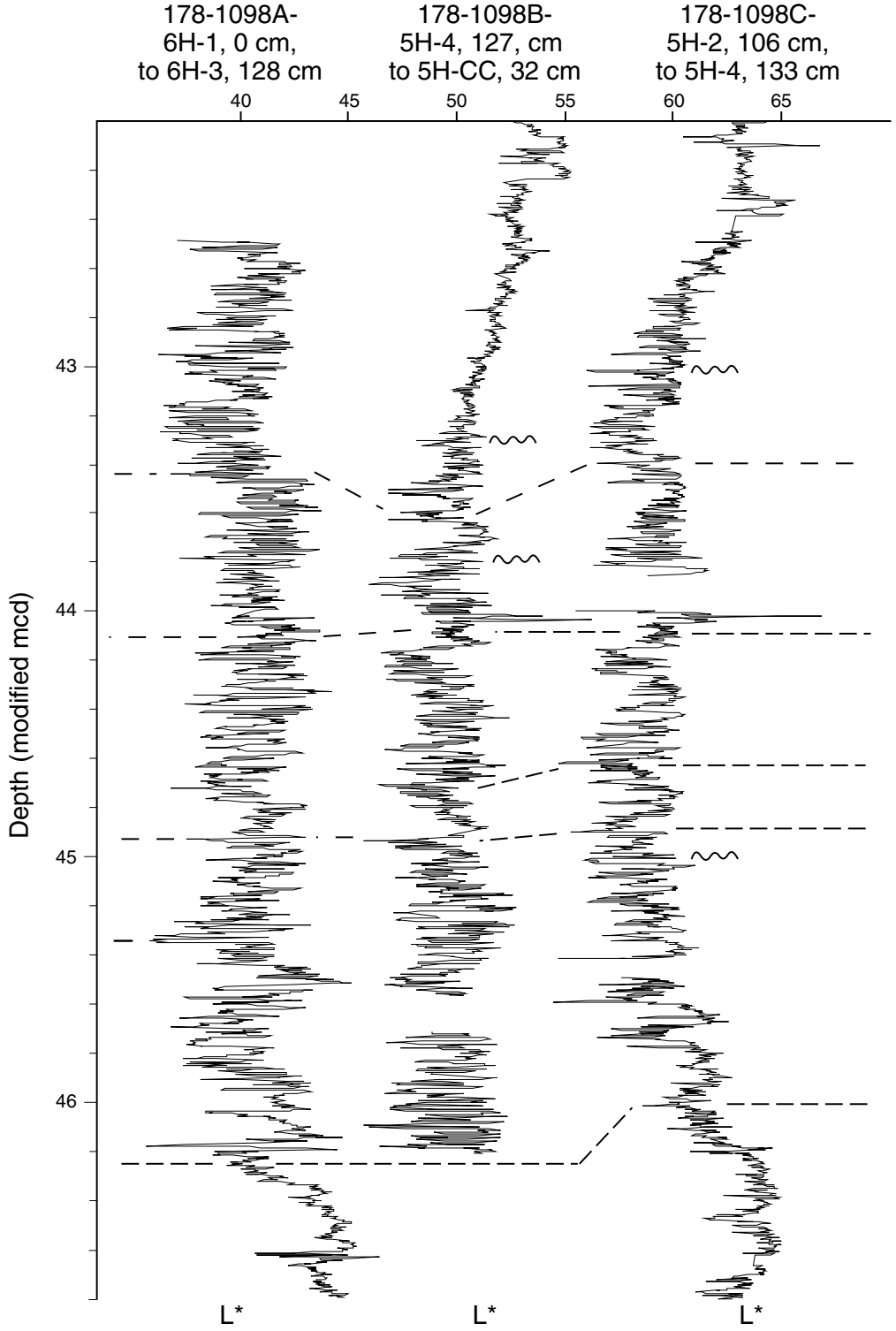

Figure F7. Image data for Holes 1098A, 1098B, and 1098C, corresponding to the interval around 44.1 mcd in Figure F6, p. 15. Holes 1098B and 1098C show a good correlation in this interval. The interval in Hole 1098A represents the best-guess correlation but shows a different pattern of lamination. Note that images are a gray-scale translation of the original color files and that contrast and brightness are enhanced.

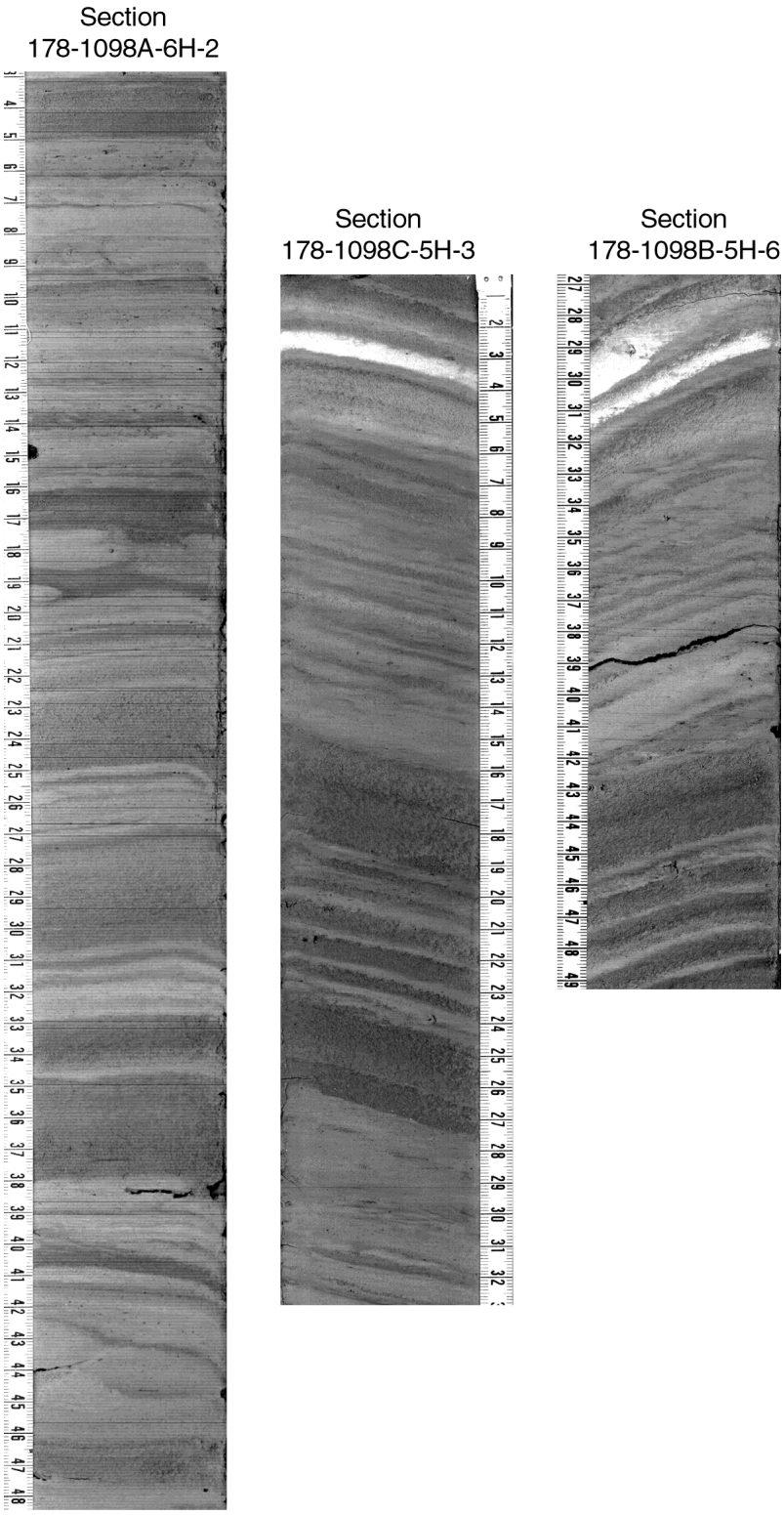

Figure F8. Thicknesses of dark/light couplets and light intervals compared to long-term average sediment accumulation rates. **A.** Thickness of dark/light couplets in the spliced record of Figure F3, p. 12, against composite depth, with total sediment accumulation rates derived from a ninth-degree polynomial fitted to the radiocarbon data of Domack et al. (in press). Note that dark/light couplets include sediment intervals between dark laminae separated by bioturbated sediments. **B.** Histogram of data in A, showing couplets ≤3 cm only; the thick dark line represents the linear average of sedimentation rates. **C.** Thicknesses of light-colored laminae and intervals only, with sedimentation rates as in A recalculated after subtraction of all dark laminae. **D.** Histogram of data in C, with linear average accumulation rate for light sediments.

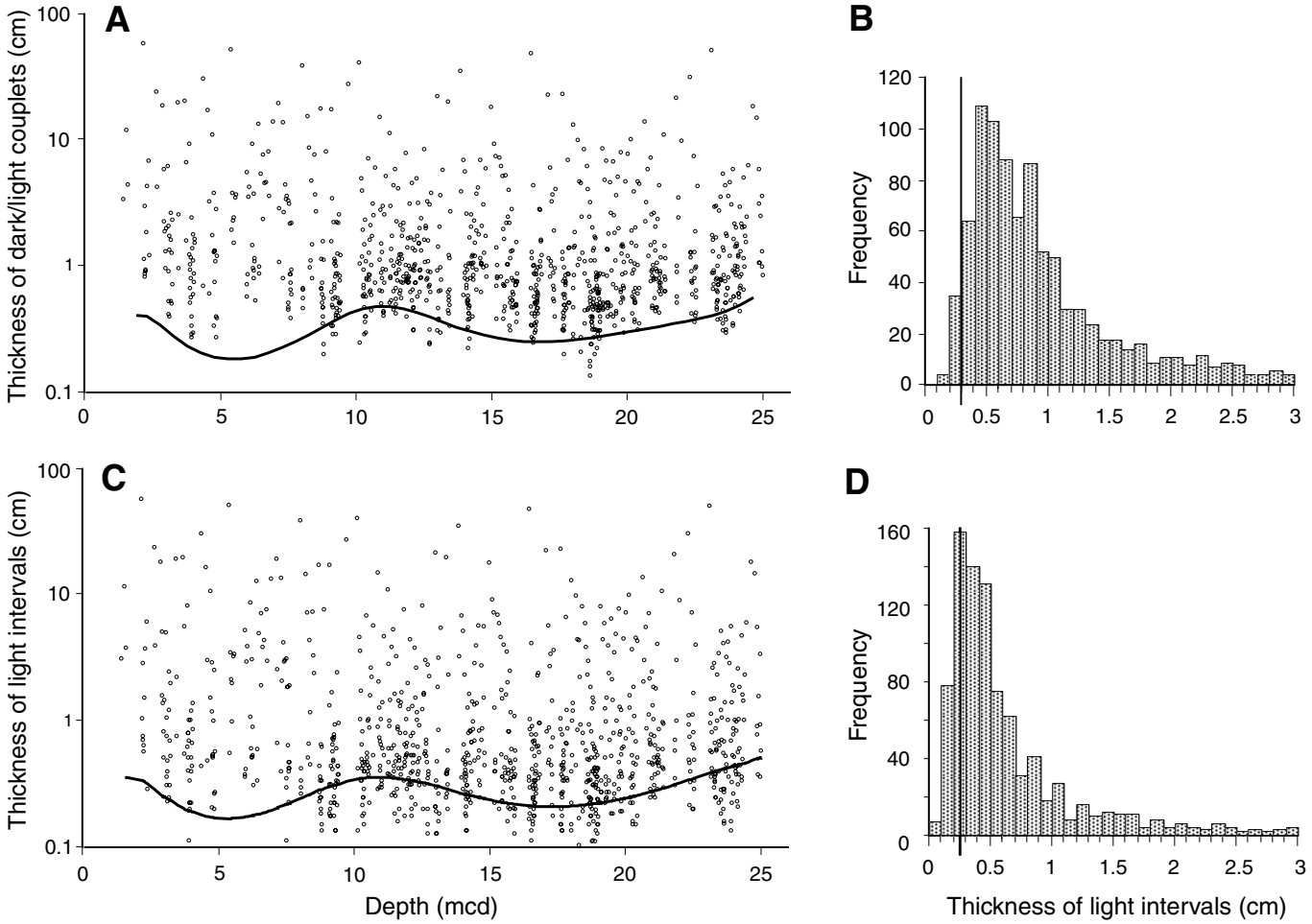

Table T1. Hole 1098A digital image color data.

Hole	Core	Section	Top interval (cm)	Bottom interval (cm)	Depth (modified mcd)	L*	a*	b*
1098A	1	1	17	18	18.5	41.6	–7.7	16.6
1098A	1	1	18	19	19.5	40.9	–7.6	16.7
1098A	1	1	19	20	20.5	40.0	–7.6	16.7
1098A	1	1	20	21	21.5	40.5	–7.6	16.5
1098A	1	1	21	22	22.5	41.5	–7.7	16.6
1098A	1	1	22	23	23.5	41.3	–7.9	16.5
1098A	1	1	23	24	24.5	40.6	–7.8	16.2
1098A	1	1	24	25	25.5	41.1	–7.9	16.3
1098A	1	1	25	26	26.5	42.0	–8.1	16.5
1098A	1	1	26	27	27.5	41.3	–7.8	16.8
1098A	1	1	27	28	28.5	41.1	–7.9	16.4
1098A	1	1	28	29	29.5	42.0	–7.9	16.7
1098A	1	1	29	30	30.5	41.6	–7.7	16.6
1098A	1	1	30	31	31.5	41.6	–7.9	16.4
1098A	1	1	31	32	32.5	41.4	–7.6	17.0
1098A	1	1	32	33	33.5	41.4	–7.8	16.9
1098A	1	1	33	34	34.5	41.4	–7.7	16.6
1098A	1	1	34	35	35.5	41.7	–7.9	17.0
1098A	1	1	35	36	36.5	41.0	–7.6	16.9
1098A	1	1	36	37	37.5	41.8	–7.9	16.7
1098A	1	1	37	38	38.5	41.6	–7.8	16.7
1098A	1	1	38	39	39.5	41.3	–7.6	16.7
1098A	1	1	39	40	40.5	41.5	–7.8	16.5
1098A	1	1	40	41	41.5	41.7	–8.0	16.8
1098A	1	1	41	42	42.5	41.9	–8.1	16.7
1098A	1	1	42	43	43.5	41.6	–8.0	16.7
1098A	1	1	43	44	44.5	42.6	–8.1	16.4
1098A	1	1	44	45	45.5	42.4	–8.1	16.6
1098A	1	1	45	46	46.5	42.6	–8.0	16.8
1098A	1	1	46	47	47.5	42.3	–8.0	16.7
1098A	1	1	47	48	48.5	41.6	–7.8	16.7
1098A	1	1	48	49	49.5	42.1	–8.0	16.3
1098A	1	1	49	50	50.5	43.1	–8.1	16.1
1098A	1	1	50	51	51.5	41.2	–7.8	16.6
1098A	1	1	51	52	52.5	40.9	–7.7	16.6
1098A	1	1	52	53	53.5	41.5	–7.8	16.5
1098A	1	1	53	54	54.5	41.5	–7.7	16.4
1098A	1	1	54	55	55.5	41.5	–7.7	16.4
1098A	1	1	55	56	56.5	41.6	–7.8	16.3
1098A	1	1	56	57	57.5	41.1	–7.6	16.4
1098A	1	1	57	58	58.5	41.9	–7.7	16.4
1098A	1	1	58	59	59.5	41.5	–7.6	16.4
1098A	1	1	59	60	60.5	41.6	–7.7	16.4
1098A	1	1	60	61	61.5	42.9	–7.9	16.0
1098A	1	1	61	62	62.5	41.3	–7.8	16.4
1098A	1	1	62	63	63.5	40.8	–7.6	16.5
1098A	1	1	63	64	64.5	41.3	–7.7	16.5
1098A	1	1	64	65	65.5	41.0	–7.7	16.6
1098A	1	1	65	66	66.5	41.0	–7.8	16.8
1098A	1	1	66	67	67.5	41.1	–7.8	16.7
1098A	1	1	67	68	68.5	41.5	–7.7	16.4
1098A	1	1	68	69	69.5	41.9	–8.0	16.3
1098A	1	1	69	70	70.5	42.2	–8.1	15.9
1098A	1	1	70	71	71.5	42.2	–8.1	16.0
1098A	1	1	71	72	72.5	42.3	–8.3	16.0
1098A	1	1	72	73	73.5	42.5	–8.1	16.2
1098A	1	1	73	74	74.5	43.0	–8.4	15.9
1098A	1	1	74	75	75.5	43.1	–8.2	16.1
1098A	1	1	75	76	76.5	42.0	–8.1	16.4
1098A	1	1	76	77	77.5	42.3	–8.2	16.1
1098A	1	1	77	78	78.5	42.6	–8.3	16.0
1098A	1	1	78	79	79.5	42.5	–8.3	16.2
1098A	1	1	79	80	80.5	42.1	–8.2	16.1
1098A	1	1	80	81	81.5	42.3	–8.3	16.0
1098A	1	1	81	82	82.5	42.0	–8.2	16.2
1098A	1	1	82	83	83.5	42.8	–8.3	16.0

Note: Only a portion of this table appears here. The complete table is available in **ASCII format**.

Table T2. Hole 1098B digital image color data.

Hole	Core	Section	Top interval (cm)	Bottom interval (cm)	Depth (modified mcd)	L*	a*	b*
1098B	1	1	2	3	9.5	41.8	–8.1	15.0
1098B	1	1	3	4	10.5	42.1	–8.0	15.0
1098B	1	1	4	5	11.5	41.9	–7.9	14.9
1098B	1	1	5	6	12.5	42.3	–7.9	15.2
1098B	1	1	6	7	13.5	41.1	–7.7	15.2
1098B	1	1	7	8	14.5	40.7	–7.8	15.3
1098B	1	1	8	9	15.5	40.9	–7.9	15.2
1098B	1	1	9	10	16.5	40.7	–7.9	15.2
1098B	1	1	10	11	17.5	41.3	–7.9	15.0
1098B	1	1	11	12	18.5	41.4	–7.9	14.9
1098B	1	1	12	13	19.5	41.5	–8.0	14.9
1098B	1	1	13	14	20.5	41.5	–8.1	15.0
1098B	1	1	14	15	21.5	41.9	–8.1	14.8
1098B	1	1	15	16	22.5	41.6	–8.1	15.1
1098B	1	1	16	17	23.5	42.0	–8.1	15.4
1098B	1	1	17	18	24.5	42.3	–8.4	15.5
1098B	1	1	18	19	25.5	42.0	–8.2	15.1
1098B	1	1	19	20	26.5	42.5	–8.4	15.4
1098B	1	1	20	21	27.5	42.6	–8.3	15.4
1098B	1	1	21	22	28.5	42.4	–8.3	15.3
1098B	1	1	22	23	29.5	42.6	–8.2	15.4
1098B	1	1	23	24	30.5	43.0	–8.4	15.6
1098B	1	1	24	25	31.5	42.6	–8.2	15.4
1098B	1	1	25	26	32.5	42.7	–8.5	15.5
1098B	1	1	26	27	33.5	42.6	–8.3	15.7
1098B	1	1	27	28	34.5	42.7	–8.2	15.6
1098B	1	1	28	29	35.5	42.3	–8.1	15.4
1098B	1	1	29	30	36.5	42.3	–8.1	15.4
1098B	1	1	30	31	37.5	42.8	–8.0	15.8
1098B	1	1	31	32	38.5	42.1	–8.1	15.8
1098B	1	1	32	33	39.5	42.2	–8.4	16.4
1098B	1	1	33	34	40.5	42.7	–8.6	15.9
1098B	1	1	34	35	41.5	42.9	–8.6	15.5
1098B	1	1	35	36	42.5	42.6	–8.3	15.3
1098B	1	1	36	37	43.5	42.7	–8.5	15.6
1098B	1	1	37	38	44.5	42.7	–8.4	15.3
1098B	1	1	38	39	45.5	42.5	–8.3	15.2
1098B	1	1	39	40	46.5	43.0	–8.5	15.2
1098B	1	1	40	41	47.5	43.1	–8.6	15.5
1098B	1	1	41	42	48.5	43.0	–8.3	15.1
1098B	1	1	42	43	49.5	42.5	–8.4	15.0
1098B	1	1	43	44	50.5	43.0	–8.6	14.7
1098B	1	1	44	45	51.5	41.8	–8.2	15.6
1098B	1	1	45	46	52.5	42.7	–8.4	15.2
1098B	1	1	46	47	53.5	42.4	–8.4	15.1
1098B	1	1	47	48	54.5	42.2	–8.4	15.2
1098B	1	1	48	49	55.5	42.5	–8.6	15.4
1098B	1	1	49	50	56.5	43.2	–8.6	14.9
1098B	1	1	50	51	57.5	44.0	–8.6	14.4
1098B	1	1	51	52	58.5	41.9	–8.3	15.0
1098B	1	1	52	53	59.5	41.4	–8.2	15.1
1098B	1	1	53	54	60.5	42.2	–8.4	15.2
1098B	1	1	54	55	61.5	42.5	–8.4	15.0
1098B	1	1	55	56	62.5	41.7	–8.3	15.1
1098B	1	1	56	57	63.5	41.1	–8.1	15.3
1098B	1	1	57	58	64.5	40.7	–8.1	15.5
1098B	1	1	58	59	65.5	41.5	–8.2	15.7
1098B	1	1	59	60	66.5	40.9	–8.0	16.1
1098B	1	1	60	61	67.5	41.2	–8.2	15.9
1098B	1	1	61	62	68.5	40.9	–8.0	15.8
1098B	1	1	62	63	69.5	42.3	–8.5	15.2
1098B	1	1	63	64	70.5	42.3	–8.4	15.1
1098B	1	1	64	65	71.5	42.4	–8.2	14.6
1098B	1	1	65	66	72.5	42.3	–8.4	14.9
1098B	1	1	66	67	73.5	42.2	–8.5	15.2
1098B	1	1	67	68	74.5	41.6	–8.2	15.2

Note: Only a portion of this table appears here. The complete table is available in **ASCII format**.

Table T3. Hole 1098C digital image color data.

Hole	Core	Section	Top interval (cm)	Bottom interval (cm)	Depth (modified mcd)	L*	a*	b*
1098C	1	2	1	2	142.5	42.1	–8.1	15.9
1098C	1	2	2	3	143.5	43.0	–8.2	15.7
1098C	1	2	3	4	144.5	42.6	–8.1	15.7
1098C	1	2	4	5	145.5	42.9	–8.2	15.8
1098C	1	2	5	6	146.5	43.1	–8.1	15.9
1098C	1	2	6	7	147.5	43.0	–8.3	16.0
1098C	1	2	7	8	148.5	42.9	–8.0	16.1
1098C	1	2	8	9	149.5	41.8	–7.9	16.3
1098C	1	2	9	10	150.5	42.2	–8.1	16.2
1098C	1	2	10	11	151.5	43.1	–8.2	16.0
1098C	1	2	11	12	152.5	43.0	–8.4	15.9
1098C	1	2	12	13	153.5	42.9	–8.3	15.9
1098C	1	2	13	14	154.5	42.9	–8.5	16.0
1098C	1	2	14	15	155.5	41.3	–8.3	16.7
1098C	1	2	15	16	156.5	41.5	–8.2	16.7
1098C	1	2	16	17	157.5	41.7	–8.1	16.6
1098C	1	2	17	18	158.5	42.0	–8.2	16.4
1098C	1	2	18	19	159.5	41.9	–8.2	16.4
1098C	1	2	19	20	160.5	41.6	–8.1	16.6
1098C	1	2	20	21	161.5	41.7	–8.2	16.8
1098C	1	2	21	22	162.5	42.1	–8.3	16.8
1098C	1	2	22	23	163.5	42.7	–8.4	16.5
1098C	1	2	23	24	164.5	42.3	–8.0	16.8
1098C	1	2	24	25	165.5	41.6	–8.1	16.9
1098C	1	2	25	26	166.5	41.6	–8.0	16.6
1098C	1	2	26	27	167.5	40.7	–7.9	16.9
1098C	1	2	27	28	168.5	40.5	–7.8	17.0
1098C	1	2	28	29	169.5	40.8	–7.9	17.0
1098C	1	2	29	30	170.5	41.3	–7.9	16.7
1098C	1	2	30	31	171.5	41.4	–8.0	16.8
1098C	1	2	31	32	172.5	41.9	–8.0	16.7
1098C	1	2	32	33	173.5	42.5	–8.1	15.9
1098C	1	2	33	34	174.5	42.1	–7.9	16.1
1098C	1	2	34	35	175.5	41.3	–7.7	16.4
1098C	1	2	35	36	176.5	42.1	–8.0	15.8
1098C	1	2	36	37	177.5	42.1	–8.2	16.0
1098C	1	2	37	38	178.5	42.0	–8.0	16.1
1098C	1	2	38	39	179.5	42.1	–8.0	15.9
1098C	1	2	39	40	180.5	41.8	–8.1	15.6
1098C	1	2	40	41	181.5	42.0	–8.0	15.9
1098C	1	2	41	42	182.5	42.1	–8.0	15.9
1098C	1	2	42	43	183.5	41.3	–7.9	15.8
1098C	1	2	43	44	184.5	39.9	–7.9	15.3
1098C	1	2	44	45	185.5	41.4	–7.7	16.5
1098C	1	2	45	46	186.5	41.7	–7.8	16.1
1098C	1	2	46	47	187.5	40.6	–7.7	15.9
1098C	1	2	47	48	188.5	40.9	–7.9	15.9
1098C	1	2	48	49	189.5	40.9	–7.7	16.1
1098C	1	2	49	50	190.5	41.2	–7.7	15.8
1098C	1	2	50	51	191.5	40.5	–7.7	16.6
1098C	1	2	51	52	192.5	40.6	–7.8	16.7
1098C	1	2	52	53	193.5	41.1	–7.9	16.4
1098C	1	2	53	54	194.5	41.2	–7.9	16.4
1098C	1	2	54	55	195.5	40.9	–7.7	16.4
1098C	1	2	55	56	196.5	41.0	–7.7	16.4
1098C	1	2	56	57	197.5	42.9	–8.1	15.7
1098C	1	2	57	58	198.5	42.0	–7.9	16.0
1098C	1	2	58	59	199.5	41.5	–7.9	15.9
1098C	1	2	59	60	200.5	42.0	–8.0	15.5
1098C	1	2	60	61	201.5	42.1	–8.1	15.6
1098C	1	2	61	62	202.5	41.4	–8.1	15.5
1098C	1	2	62	63	203.5	40.8	–7.9	16.0
1098C	1	2	63	64	204.5	41.2	–7.9	16.1
1098C	1	2	64	65	205.5	41.4	–7.9	16.2
1098C	1	2	65	66	206.5	42.4	–8.2	16.0
1098C	1	2	66	67	207.5	41.5	–8.2	16.3

Note: Only a portion of this table appears here. The complete table is available in **ASCII format**.